Polarized Raman scattering studies of crystal-field excitations in $ErNi_2B_2C$

H. Rho,[1,2] M. V. Klein,[1] and P. C. Canfield[3]
[1]*Department of Physics and Frederick Seitz Materials Research Laboratory, University of Illinois at Urbana-Champaign, Urbana, Illinois 61801, USA*
[2]*Department of Physics, Chonbuk National University, Jeonju 561-756, Korea*
[3]*Ames Laboratory, Department of Physics and Astronomy, Iowa State University, Ames, Iowa 50011, USA*
(Received 3 December 2003; published 20 April 2004)

Raman-scattering measurements have been carried out to study magnetic properties of the quaternary magnetic superconductor $ErNi_2B_2C$ ($T_c=10$ K, $T_N=6$ K). The crystal field (CF) of Er^{3+} splits the 16-fold degenerate $^4I_{15/2}$ ground-state multiplet of $4f^{11}$ electrons into eight Kramers doublets $4\Gamma_6+4\Gamma_7$ within the D_{4h} site symmetry. Therefore, one expects seven ground-state CF transitions from the lowest Γ_6 state to the higher states. Excitation symmetries and transition characteristics between these levels can be identified systematically by a proper use of the Raman polarization selection rules. As a result, temperature-dependent and polarized Raman-scattering spectra reveal six ground-state CF transitions: 7 cm^{-1} ($\Gamma_6\rightarrow\Gamma_7$), 48 cm^{-1} ($\Gamma_6\rightarrow\Gamma_6$), 56 cm^{-1} ($\Gamma_6\rightarrow\Gamma_7$), 145 cm^{-1} ($\Gamma_6\rightarrow\Gamma_7$), 149 cm^{-1} ($\Gamma_6\rightarrow\Gamma_6$), and 153 cm^{-1} ($\Gamma_6\rightarrow\Gamma_7$). Using the CF transition characteristics of the obtained data, we expect that one unobserved CF level transition ($\Gamma_6\rightarrow\Gamma_6$) lies between 56 cm^{-1} and 145 cm^{-1}.

DOI: 10.1103/PhysRevB.69.144420 PACS number(s): 75.30.−m, 78.30.−j, 74.70.Dd, 71.70.Ch

I. INTRODUCTION

The magnetic rare-earth borocarbide superconductors RNi_2B_2C (R=Tm, Er, Ho, Dy) have attracted a great deal of interest due to the strong correlations between superconductivity and magnetism.[1–11] Effects of the magnetic moments at the rare-earth sites on the superconductivity in these materials exhibit exotic behavior governing the interplay between superconductivity and magnetism. Both the superconducting transition temperatures (T_c) and the antiferromagnetic-ordering temperatures (T_N) of RNi_2B_2C are systematically scaled by the de Gennes factor, indicating that the itinerant electrons are weakly coupled to the localized $4f$ electrons of the rare-earth ions, and both T_c and T_N originate from the same conduction electron-local magnetic moment exchange interactions.[1,2] In contrast to the mutually exclusive nature between superconductivity and magnetism, experimental evidences of coexistence of these two phenomena in RNi_2B_2C elucidate a new understanding of magnetic properties in the superconducting state as well as in the normal state. For instance, transport and neutron measurements in $ErNi_2B_2C$ reveal that superconductivity coexists not only with antiferromagnetism for $T<\sim 6$ K (Refs. 1,3–5) but also with spontaneous weak ferromagnetism for $T<2.3$ K.[6]

Studies of the crystal-field (CF) excitations provide useful information on the magnetic properties of superconducting materials. The CF interactions are primarily responsible for the strong magnetic anisotropies observed in the normal states of RNi_2B_2C (Refs. 2,7–9) and RRh_4B_4 (Ref. 12) as well as the Schottky anomalies observed in the specific heat measurements.[8,13–15] The highly anisotropic nature of the local moments strongly influences the interplay between the superconductivity and the magnetism, and for these reasons active investigations of the CF excitations have been carried out for RNi_2B_2C using various experimental techniques such as inelastic neutron scattering,[14–18] Mössbauer spectroscopy,[19] and Raman-scattering[20] measurements.

Inelastic (Raman) scattering provides useful means to simultaneously probe electronic and phononic excitations.[21] By controlling polarization directions of the incident and scattered light, the Raman polarization selection rules allow one to identify the symmetry information of a particular excitation. Raman-scattering studies of RNi_2B_2C have been performed on optical phonons in RNi_2B_2C (R=Lu, Ho, Y),[22,23] low-frequency electronic excitations in YNi_2B_2C,[24] and superconducting gaps in RNi_2B_2C (R=Y, Lu).[25,26]

In this paper, we use polarized Raman scattering to explore scattering symmetries and transition characteristics of the CF excitations in superconducting $ErNi_2B_2C$ in the temperature range 4–300 K. Using a triple-spectrometer system uniquely designed for high-stray-light rejection and high throughput, we obtained six CF excitations and identified each scattering symmetry. The observed CF excitations include a low-lying CF excitation at 7 cm^{-1} ($\sim$0.86 meV) proposed by Bonville *et al.*[19] based on their specific-heat measurements. Note that previous inelastic neutron-scattering[14,15,17] and Raman-scattering[20] measurements from $ErNi_2B_2C$ revealed only a few CF excitations.

II. EXPERIMENT

A single crystal $ErNi_2B_2C$ sample[8,11] was mounted inside a continuous Helium-flow cryostat with a variable-temperature option. Raman-scattering measurements were performed in a backscattering geometry along the growth (c axis) direction of the sample using a Kr-ion laser with the 647.1 nm excitation wavelength. Linearly or circularly polarized light was employed in various polarization configurations to identify the scattering symmetries for $ErNi_2B_2C$: $z(x,x)\bar{z}$, $B_{1g}+A_{1g}$; $z(x,y)\bar{z}$, $B_{2g}+A_{2g}$; $z(x',x')\bar{z}$, $B_{2g}+A_{1g}$; $z(x',y')z$, $B_{1g}+A_{2g}$; $z(L,L)\bar{z}$, $A_{1g}+A_{2g}$; $z(L,R)\bar{z}$, $B_{1g}+B_{2g}$, where B_{1g}, B_{2g}, A_{1g}, and A_{2g} are irreducible representations (IR's) of the space group D_{4h}. In

the notation of $z(x,y)\bar{z}$, z and $\bar{z}$ represent wave-vector directions of the incident and scattered light, respectively, (x,y) represents the polarization directions of the incident and analyzed (i.e., scattered) light, respectively, and $x\|[1,0,0]$, $y\|[0,1,0]$, and $z\|[0,0,1]$. Symbols x' and y' represent two mutually orthogonal directions parallel to $[1,1,0]$ and $[-1,1,0]$, respectively. Symbols L and R represent left and right circularly polarized light, respectively. Scattered light was dispersed through a triple spectrometer equipped with an 1800 g/mm grating, and recorded using a liquid-nitrogen-cooled charge-coupled device (CCD) detector. All the spectra were corrected, first, by removing the CCD dark current response, and then by normalizing the spectrometer response using a calibrated white light source. Finally, the corrected spectra were divided by the Bose thermal factor $[1-\exp(-\hbar\omega/k_BT)]^{-1}$, giving rise to the resultant spectra proportional to the imaginary part of the Raman susceptibility.

III. RESULTS AND DISCUSSION

The rare-earth nickel borocarbide single crystals have the body-centered-tetragonal structure with space group D_{4h}^{17}-$I4/mmm$.[27] The ground state of the 11 $4f$ electrons ($4f^{11}$) in Er^{3+} is 16-fold degenerate $^4I_{15/2}$. The total angular momentum $J=15/2$ comes from the spin-orbit coupling: the angular momentum $L=6$ and the spin $S=3/2$. Within the D_{4h} site symmetry at the Er site, the CF level splits the ground-state multiplet into eight Kramers doublets $4\Gamma_6+4\Gamma_7$, where Γ's are IR's of the group D_{4h}.[28] Therefore, one expects seven ground-state CF transitions in $ErNi_2B_2C$ between the lowest and higher CF levels. Electronic transitions between these levels are governed in decomposition of the direct products of Γ_6 and Γ_7 with the four IR's discussed in Sec. II above:

$$B_{1g}\times\Gamma_{6,7}=B_{2g}\times\Gamma_{6,7}=\Gamma_{7,6}, \quad (1)$$

$$A_{1g}\times\Gamma_{6,7}=A_{2g}\times\Gamma_{6,7}=\Gamma_{6,7}. \quad (2)$$

Polarized Raman scattering with B_{1g} or B_{2g} symmetry corresponds to electronic transitions $\Gamma_6\rightarrow\Gamma_7$ and $\Gamma_7\rightarrow\Gamma_6$. Likewise, polarized Raman scattering with A_{1g} or A_{2g} symmetry corresponds to electronic transitions $\Gamma_6\rightarrow\Gamma_6$ and $\Gamma_7\rightarrow\Gamma_7$. In this way, the CF excitation symmetries and their transition characteristics can be identified.

Figure 1(a) illustrates the $B_{1g}+A_{2g}$ Raman-scattering spectra of $ErNi_2B_2C$ with increasing temperature from top to bottom. The strong spectral peak at ~ 199 cm^{-1} is assigned to the B_{1g} phonon mode from the c-axis Ni vibration.[22,23] In addition to the Ni-B_{1g} phonon mode, numerous Raman excitations were observed. With increasing temperature, the additional Raman responses broaden and weaken in spectral weight. Finally, above $T=260$ K, the Raman responses were weak as to be barely observable. These features are characteristics of the CF excitations, as observed in the high-T_c superconductors and their parent compounds containing rare-earth atoms.[29,30] Indeed, the electronic Raman peaks at 48 cm^{-1} and 145 cm^{-1} are very close to the CF transitions

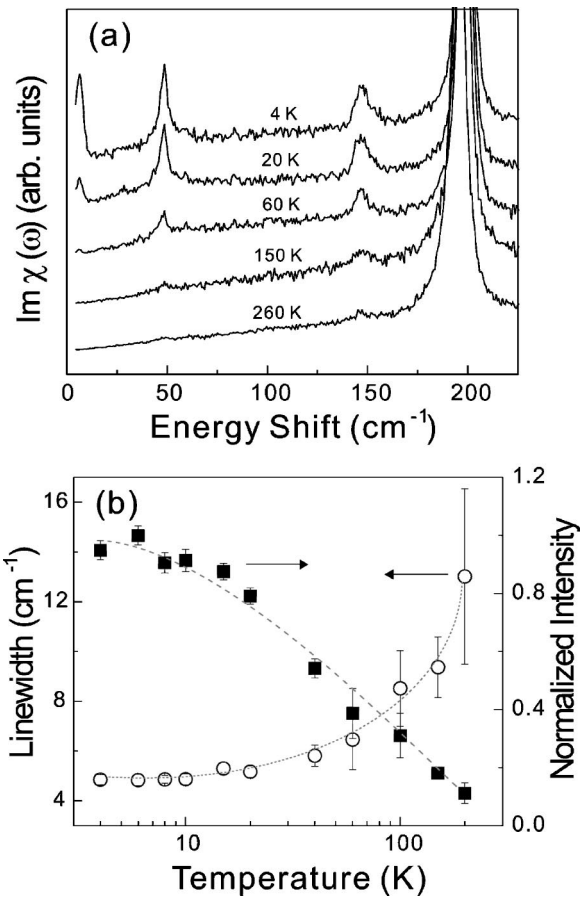

FIG. 1. (a) Temperature evolution of the $B_{1g}+A_{2g}$ Raman-scattering spectra of $ErNi_2B_2C$ upon heating from top to bottom. A strong Raman response at ~ 199 cm^{-1} is the Ni-B_{1g} phonon response. (b) Summary of the spectral linewidth changes (open circles) and the corresponding normalized spectral intensity changes (filled squares) of the 48 cm^{-1} CF excitation response, respectively, as a function of temperature. The dotted and dashed lines are guides to the eye.

observed in inelastic neutron-scattering[17] and Raman-scattering[20] measurements from $ErNi_2B_2C$. Figure 1(b) summarizes the spectral linewidth and normalized intensity changes, obtained from fits to a Lorentzian profile, for the 48 cm^{-1} CF transition with increasing temperature. The spectral linewidth and intensity start to broaden and weaken, respectively, for $T>\sim T_N$, clearly demonstrating that this Raman response is electronic in origin and reflects a CF excitation. Likewise, all the other CF excitations show the same behavior as a function of temperature. Note that, in comparison to the previous Raman-scattering results,[20] the $B_{1g}+A_{2g}$ Raman spectra in Fig. 1(a) exhibit at least two additional CF excitations at 7 cm^{-1} and 56 cm^{-1} shown more clearly in Fig. 2 and discussed below.

The eight CF levels in $ErNi_2B_2C$ consist of Γ_6, Γ_7, Γ_6, Γ_7, Γ_6, Γ_7, Γ_6, and Γ_7 from the lowest doublet ground state to the higher doublet states.[17,20] To explore the CF excitations and their transition properties in detail, we performed polarized Raman-scattering measurements in various scattering configurations. As a result, six CF excitations are

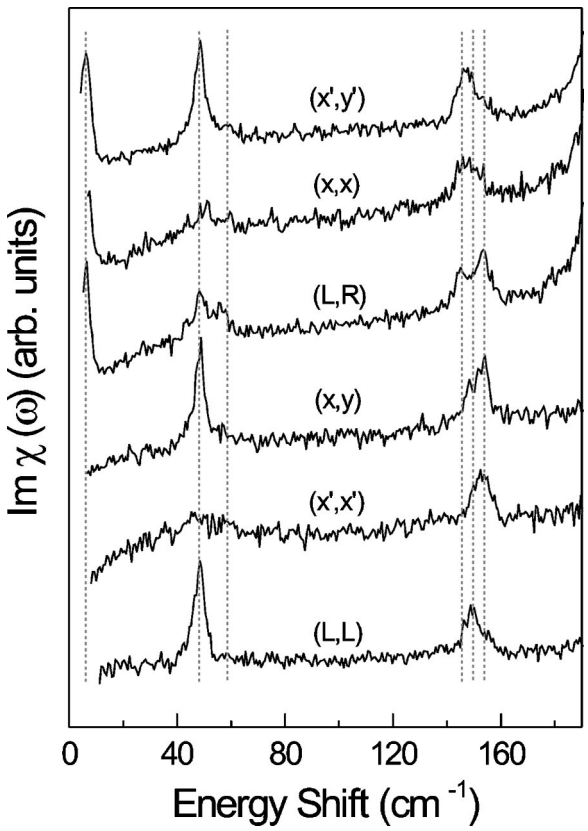

FIG. 2. Polarized Raman-scattering spectra of $ErNi_2B_2C$ at 4 K in various scattering configurations, showing six CF transitions at 7 cm^{-1}, 48 cm^{-1}, 56 cm^{-1}, 145 cm^{-1}, 149 cm^{-1}, and 153 cm^{-1}, as indicated by the dotted lines.

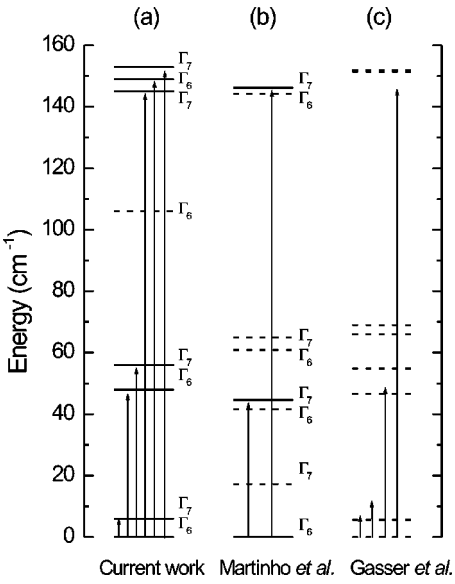

FIG. 3. (a) The CF ground-state energy level scheme and transition characteristics of the current work. The six arrows indicate the observed CF transitions. A dashed line lying between 56 cm^{-1} and 145 cm^{-1} denotes an energetic location of the unobserved CF transition. (b) The CF ground-state energy level scheme and transition characteristics by Martinho *et al*.[20] The dashed and solid lines indicate the calculated results. Two arrows indicate the Raman-scattering results. (c) The CF ground-state energy level scheme by Gasser *et al*.[17] The dashed lines indicate the calculated results. Four arrows indicate the inelastic neutron-scattering results. Two CF transitions at $\sim$6.5 cm^{-1} and $\sim$12 cm^{-1} result from splitting of the low-lying CF transition.

observed, as summarized in Fig. 2. We did not find any considerable Raman scattering response due to the CF excitations in the higher-energy region.

To identify each of the CF transition characteristics, first, consider the low-lying CF excitation at 7 cm^{-1}. Although the low-energy shoulder of this excitation was cut off $\sim$4 cm^{-1} due to the spectral limit of the spectrometer, the peak at 7 cm^{-1} was clearly resolved. Because the 7 cm^{-1} CF excitation is observed in the (x',y') scattering configuration, it has either B_{1g} or A_{2g} Raman symmetry. However, it is also observed in the (x,x) scattering configuration with $B_{1g}+A_{1g}$ Raman symmetries. Therefore, the 7 cm^{-1} CF excitation, observed in these two scattering configurations, is related neither to A_{1g} nor to A_{2g} Raman symmetry. If the 7 cm^{-1} CF excitation had the A_{1g} or the A_{2g} Raman symmetry, it would not be observed in both scattering configurations. Thus, we conclude that the 7 cm^{-1} CF excitation has B_{1g} Raman symmetry, corresponding to a CF transition from the lowest Γ_6 state to the higher Γ_7 state [see Eq. (1)]. The fact that the 7 cm^{-1} CF excitation has B_{1g} Raman symmetry is further exemplified by its appearance in the Raman spectrum obtained in the (L,R) scattering configuration with $B_{1g}+B_{2g}$ Raman symmetries. In the same way, the 145 cm^{-1} CF excitation observed in the (x',y'), (x,x), and (L,R) scattering configurations is unambiguously assigned to have B_{1g} Raman symmetry, corresponding to a $\Gamma_6 \rightarrow \Gamma_7$ CF transition. Similarly, the 48 cm^{-1} CF excitation is observed in the (x',y'), (x,y), and (L,L) scattering configurations which have A_{2g} Raman symmetry in common. Therefore, the 48 cm^{-1} CF excitation has the totally antisymmetric A_{2g} Raman symmetry, corresponding to a $\Gamma_6 \rightarrow \Gamma_6$ CF transition. Note that there is slight leakage of this mode in other scattering configurations probably due to the imperfect polarization geometry. The 153 cm^{-1} CF excitation is observed in the (L,R), (x,y), and (x',x') scattering configurations and, therefore, it has B_{2g} Raman symmetry, corresponding to a $\Gamma_6 \rightarrow \Gamma_7$ CF transition. It is not clear whether the 149 cm^{-1} CF excitation, clearly observed in the (L,L) scattering configuration, has A_{1g} or A_{2g} Raman symmetry. However, both Raman symmetries correspond to a $\Gamma_6 \rightarrow \Gamma_6$ CF transition [see Eq. (2)]. In addition, a weak CF scattering response at 56 cm^{-1} was observed with B_{1g} Raman symmetry, corresponding to a $\Gamma_6 \rightarrow \Gamma_7$ CF transition.

Figure 3(a) summarizes the results of the CF ground-state energy level scheme and transition characteristics in $ErNi_2B_2C$ obtained by our polarized Raman-scattering results. Additionally, other experimental results (up arrows) observed in Raman-scattering[20] and inelastic neutron-scattering[17] measurements are added in Figs. 3(b) and 3(c) for comparison. Note that, in comparison to the previous Raman-scattering results which identified two CF excitations, our work resolved six CF excitations. The Raman polarization selection rules and the CF transition char-

acteristics tell us that the unobserved CF excitation (Γ_6) corresponds to a $\Gamma_6 \rightarrow \Gamma_6$ CF transition and, therefore, lies between the 56 cm^{-1} (Γ_7) and the 145 cm^{-1} (Γ_7) CF levels, as indicated by a dashed line in Fig. 3(a).

IV. CONCLUSIONS

In summary, the polarized Raman-scattering measurements reveal six CF excitations with the following level scheme: 0 cm^{-1} (Γ_6), 7 cm^{-1} (Γ_7), 48 cm^{-1} (Γ_6), 56 cm^{-1} (Γ_7), 145 cm^{-1} (Γ_7), 149 cm^{-1} (Γ_6), and 153 cm^{-1} (Γ_7). Using the Raman polarization selection rules and the CF transition characteristics, we estimate that an unobserved CF doublet (Γ_6) lies between 56 cm^{-1} and 145 cm^{-1}. Our work demonstrates that a careful use of the Raman polarization selection rules allows one not only to identify the CF excitation symmetries and transition characteristics but also to obtain useful information on the unobserved CF excitations. These results should provide an excellent starting point to obtain more refined CF parameters as well as useful information on the magnetic ground states of $ErNi_2B_2C$.

ACKNOWLEDGMENTS

We thank I.-S. Yang for useful discussions. H. R. acknowledges financial support by Korea Research Foundation (Grant No. KRF-2003-002-C00101). The research at the University of Illinois was funded by the Department of Physics. Ames Laboratory is operated for the U.S. Department of Energy by Iowa State University of Science and Technology under Contract No. W-7405-ENG-82.

[1] H. Eisaki, H. Takagi, R.J. Cava, B. Batlogg, J.J. Krajewski, and W.F. Peck, Jr., K. Mizuhashi, J.O. Lee, and S. Uchida, Phys. Rev. B **50**, 647 (1994).
[2] B.K. Cho, P.C. Canfield, and D.C. Johnston, Phys. Rev. B **52**, R3844 (1995).
[3] J.W. Lynn, S. Skanthakumar, Q. Huang, S.K. Sinha, Z. Hossain, L.C. Gupta, R. Nagarajan, and C. Godart, Phys. Rev. B **55**, 6584 (1997).
[4] J. Zarestky, C. Stassis, A.I. Goldman, P.C. Canfield, P. Dervenagas, B.K. Cho, and D.C. Johnston, Phys. Rev. B **51**, 678 (1995).
[5] S.K. Sinha, J.W. Lynn, T.E. Grigereit, Z. Hossain, L.C. Gupta, R. Nagarajan, and C. Godart, Phys. Rev. B **51**, 681 (1995).
[6] S.-M. Choi, J.W. Lynn, D. Lopez, P.L. Gammel, P.C. Canfield, and S.L. Bud'ko, Phys. Rev. Lett. **87**, 107001 (2001).
[7] B.K. Cho, B.N. Harmon, D.C. Johnston, and P.C. Canfield, Phys. Rev. B **53**, 2217 (1996).
[8] B.K. Cho, P.C. Canfield, L.L. Miller, D.C. Johnston, W.P. Beyermann, and A. Yatskar, Phys. Rev. B **52**, 3684 (1995).
[9] B.K. Cho, Ming Xu, P.C. Canfield, L.L. Miller, and D.C. Johnston, Phys. Rev. B **52**, 3676 (1995).
[10] K. Nørgaard, M.R. Eskildsen, N.H. Andersen, J. Jensen, P. Hedegård, S.N. Klausen, and P.C. Canfield, Phys. Rev. Lett. **84**, 4982 (2000).
[11] P.C. Canfield, P.L. Gammel, and D.J. Bishop, Phys. Today **51**(10), 40 (1998).
[12] B.D. Dunlap, L.N. Hall, F. Behroozi, G.W. Crabtree, and D.G. Niarchos, Phys. Rev. B **29**, 6244 (1984).
[13] H.B. Radousky, B.D. Dunlap, G.S. Knapp, and D.G. Niarchos, Phys. Rev. B **27**, 5526 (1983).
[14] J.S. Gardner, C.V. Tomy, L. Afalfiz, G. Balakrishnan, D.McK. Paul, B.D. Rainford, R. Cywinski, R.S. Eccleston, and E.A. Goremychkin, Physica B **213-214**, 136 (1995).
[15] L. Afalfiz, C.V. Tomy, J.S. Gardner, E.A. Goremychkin, R.S. Eccleston, G. Balakrishnan, M.R. Lees, and D.M. Paul, Physica C **235-240**, 2555 (1994).
[16] T.E. Grigereit, J.W. Lynn, R.J. Cava, J.J. Krajewski, and W.F. Peck, Jr., Physica C **248**, 382 (1995).
[17] U. Gasser, P. Allenspach, F. Fauth, W. Henggeler, J. Mesot, A. Furrer, S. Rosenkranz, P. Vorderwisch, and M. Buchgeister, Z. Phys. B **101**, 345 (1996).
[18] J. Mesot, P. Allenspach, U. Gasser, and A. Furrer, J. Alloys Compd. **250**, 559 (1997).
[19] P. Bonville, J.A. Hodges, C. Vaast, E. Alleno, C. Godart, L.C. Gupta, Z. Hossain, R. Nagarajan, G. Hilscher, and H. Michor, Z. Phys. B **101**, 511 (1996).
[20] H. Martinho, J.A. Sanjurjo, C. Rettori, P.C. Canfield, and P.G. Pagliuso, J. Magn. Magn. Mater. **226-230**, 978 (2001).
[21] M.V. Klein, in *Light Scattering in Solids I*, 2nd ed., edited by M. Cardona (Springer-Verlag, Berlin, 1983), p. 147.
[22] V.G. Hadjiev, L.N. Bozukov, and M.G. Baychev, Phys. Rev. B **50**, 16 726 (1994).
[23] H.-J. Park, H.-S. Shin, H.-G. Lee, I.-S. Yang, W.C. Lee, B.K. Cho, P.C. Canfield, and D.C. Johnston, Phys. Rev. B **53**, 2237 (1996).
[24] A.P. Litvinchuk, L. Börjesson, N.X. Phuc, and N.M. Hong, Phys. Rev. B **52**, 6208 (1995).
[25] I.-S. Yang, M.V. Klein, S.L. Cooper, P.C. Canfield, B.K. Cho, and S.-I. Lee, Phys. Rev. B **62**, 1291 (2000).
[26] I.-S. Yang, M.V. Klein, S. Bud'ko, and P.C. Canfield, J. Phys. Chem. Solids **63**, 2195 (2002).
[27] T. Siegrist, H.W. Zandbergen, R.J. Cava, J.J. Krajewski, and W.F. Peck, Jr., Nature (London) **367**, 254 (1994).
[28] J.L. Prather, Natl. Bur. Stand. (U.S.) Monograph No. 19 (U.S. GPO, Washington, D.C., 1961).
[29] M. Cardona, Physica C **317-318**, 30 (1999).
[30] J.A. Sanjurjo, C. Rettori, S. Oseroff, and Z. Fisk, Phys. Rev. B **49**, 4391 (1994).